

Global resurfacing of Mercury 4.0–4.1 billion years ago by heavy bombardment and volcanism

Simone Marchi¹, Clark R. Chapman², Caleb I. Fassett³, James W. Head⁴, W. F. Bottke² & Robert G. Strom⁵

The most heavily cratered terrains on Mercury have been estimated to be about 4 billion years (Gyr) old^{1–4}, but this was based on images of only about 45 per cent of the surface; even older regions could have existed in the unobserved portion. These terrains have a lower density of craters less than 100 km in diameter than does the Moon^{1,3,5}, an observation attributed to preferential resurfacing on Mercury. Here we report global crater statistics of Mercury's most heavily cratered terrains on the entire surface. Applying a recent model for early lunar crater chronology⁶ and an updated dynamical extrapolation to Mercury⁷, we find that the oldest surfaces were emplaced just after the start of the Late Heavy Bombardment (LHB) about 4.0–4.1 Gyr ago. Mercury's global record of large impact basins⁸, which has hitherto not been dated, yields a similar surface age. This agreement implies that resurfacing was global and was due to volcanism, as previously suggested^{1,5}. This activity ended during the tail of the LHB, within about 300–400 million years after the emplacement of the oldest terrains on Mercury. These findings suggest that persistent volcanism could have been aided by the surge of basin-scale impacts during this bombardment.

The earliest geological features that have been detected on Mercury, the heavily cratered terrains, show signs of ancient resurfacing as shown by the intercrater smooth plains. Early work, based on partial coverage by Mariner 10 images, suggested that both volcanism¹ and basin ejecta⁹ could have been responsible for the formation of the intercrater plains. Recent work¹⁰ based on high-resolution imaging from MESSENGER (MErcury Surface, Space ENvironment, GEOchemistry, and Ranging) presented evidence that the extensive intercrater plains seen in the heavily cratered terrains resulted from an early period of volcanism, although clear volcanic sources for these ancient units have not yet been identified. The timing and areal extent of this proposed resurfacing on Mercury, and the specific role of volcanism, have been unknown.

As is true for other terrestrial bodies, except the Earth and the Moon, Mercury's relative geological chronology has been inferred from observations of the impact crater record (see, for example, ref. 11), with absolute ages then extrapolated from the better-constrained lunar crater chronology^{12–14}. Here we measure crater size–frequency distributions for the most heavily cratered terrains on Mercury to determine their absolute ages. The age of the most heavily cratered terrains is an important benchmark for Mercury, because it provides an upper limit for the formation of subsequent major geological units such as the widespread volcanic smooth plains in the annulus surrounding the Caloris basin¹⁵ and in high northern latitudes of Mercury¹⁶. The currently visible impactor population in the terrestrial planet region, namely near-Earth objects, is now well characterized for kilometre-sized asteroids¹⁷, although impact rates and size distributions are less certain for earlier epochs. By using current models of the impact rate in the inner solar system, a model production function for lunar cratering has been developed and extrapolated to Mercury⁷. More recently, an independent model¹⁸ found comparable results.

We initially identified the most heavily cratered terrains on Mercury using a preliminary global crater catalogue⁵, then defined their boundaries on a new MESSENGER global mosaic. We concentrated on two regions of high crater density (Supplementary Fig. 1): the northern heavily cratered terrains (NHCT; Fig. 1) and a heavily cratered area at southern latitudes east of Rembrandt basin unseen by Mariner 10 (Supplementary Fig. 1). The NHCT is a surviving remnant of a once larger heavily cratered terrain. Adjacent regions experienced more substantial resurfacing by the northern volcanic plains, the circum-Caloris volcanic plains, and by young basins east of the NHCT. The region east of Rembrandt was studied in a similar manner and produced comparable results (Supplementary Fig. 2), so we restrict discussion in this paper to the NHCT region.

The next step was to use a model production function of craters to model the observed cumulative number of craters at least 25 km in diameter on NHCT (see Supplementary Fig. 2). The model production function was obtained⁷ by using an impactor size–frequency distribution resembling that of the main asteroid belt^{7,19,20}, which has provided a suitable fit to old units on Mercury, the Moon and Mars. As can be seen, the model production function fits the NHCT data quite well, ensuring that our model is well suited to studying the early cratering on Mercury.

Cratering data for the northern heavily cratered terrains are plotted in both cumulative and *R*-plot formats²¹ in Fig. 2. The associated lunar data come from crater counts on specific ancient lunar terrains²⁰. The pre-Nectarian terrains were defined as a particular portion of the northern farside highlands. They represent one of the oldest lunar terrains, with a crater spatial density that slightly exceeds that of the NHCT on Mercury. The post-Nectarian crater size–frequency distribution is representative of terrains coeval with or younger than the Nectaris basin, a stratigraphic benchmark in lunar history²².

In general, we find that the spatial density of craters from the lunar and Mercurian terrains in Fig. 2b approaches empirical saturation equilibrium, which is thought to occur at $R = 0.2–0.3$, for diameters near 100 km (ref. 23), but they fall well below this level for craters that are considerably larger or smaller. The shapes of the NHCT and lunar pre-Nectarian terrains crater size–frequency distributions also resemble that of the lunar nearside highlands crater size–frequency distribution^{1,20}. The question is whether these ancient units have reached crater saturation or whether they still represent the size–frequency distribution of the impactor population. The characteristics of the crater size–frequency distributions on the NHCT and pre-Nectarian terrains lead us to adopt the view that those terrains are in production (see Supplementary Information for discussion).

To interpret the ancient crater size–frequency distribution on Mercury within the context of lunar chronology, we need to account for the differences between Mercury and the Moon concerning impact velocities, gravitational focusing and other factors that affect crater scaling relationships. Using the current Moon-crossing and Mercury-crossing asteroid populations derived from ref. 24, we find that on average

¹NASA Lunar Science Institute, Southwest Research Institute, Boulder, Colorado 80302, USA. ²Southwest Research Institute, Boulder, Colorado 80302, USA. ³Department of Astronomy, Mount Holyoke College, South Hadley, Massachusetts 01075, USA. ⁴Department of Geological Sciences, Brown University, Providence, Rhode Island 02912, USA. ⁵Department of Planetary Sciences, University of Arizona, Tucson, Arizona 85721, USA.

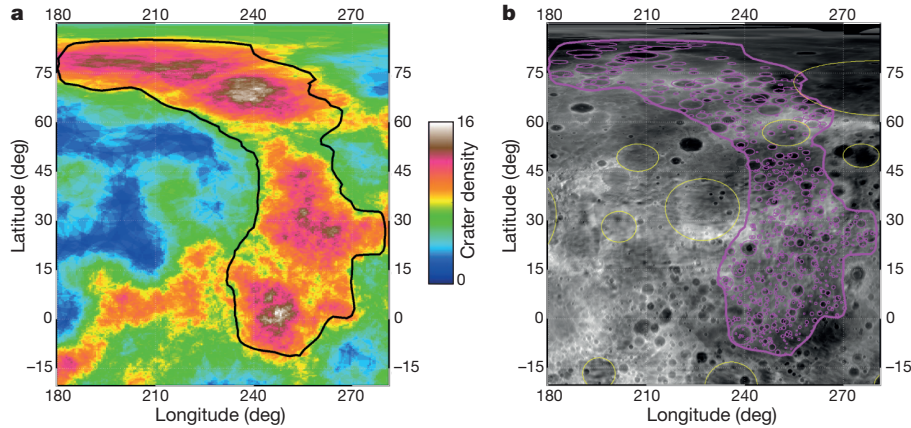


Figure 1 | The northern heavily cratered terrains of Mercury. Crater measurements were made from a global mosaic with a resolution of 500 m per pixel based on MESSENGER images obtained during its first year orbiting Mercury. Our reliance on the global mosaic for actual crater measurements was augmented, for a few regions of poorer imaging and for some highly degraded craters, by a global digital terrain model having a resolution of about 1,300 m per pixel produced from wide-angle camera images by R. Gaskell (personal communication, 2012). **a**, Crater areal density (in number of craters at least 25 km in diameter per 10^5 km^2) obtained by averaging over a radius of 300 km.

about 3–3.5-fold as many craters in the size range relevant for this work (20–300 km) should form on Mercury as on the Moon (Supplementary Fig. 3). In this work we adopt a conservative factor of 3 (valid at 20 km), a value consistent with an independent estimate¹⁸. Furthermore, we adopted a recently revised early lunar chronology⁶ for ages older than 3 Gyr (Fig. 3). The earliest declining lunar bombardment was due to planetesimals left over from terrestrial planet formation. Beginning about 4.1 Gyr ago there was a spike in the bombardment rate (the LHB) due to asteroids ejected from the primordial asteroid belt by sweeping resonances in the wake of late giant planet migration²⁵, which declined over at least the subsequent 0.6 Gyr. This is manifested in the cumulative plot by the break in slope at 4.1 Gyr ago. We also plot in Fig. 3

Smaller craters were not included in the analysis because they can be heavily affected by secondary cratering and erasure (see, for example, ref. 15). The black line defines the northern heavily cratered terrains used in this paper. Although there are small regions within the outlined region of somewhat higher crater density, these may be statistical fluctuations and in any case would be such small counting areas that the statistics would be poor. **b**, Measured craters at least 25 km diameter (pink circles) overlaid on the digital terrain model. Basins at least 300 km in diameter are indicated by yellow circles. Only one such basin has been incorporated into the crater size–frequency distribution.

the expected cumulative cratering flux for Mercury, appropriately scaled by the factor discussed above. The results show that the NHCT has an age of about 4.0–4.1 Gyr and therefore is likely to be several hundreds of million years younger than the most ancient lunar terrains (interpreted in ref. 6 to be about 4.4 Gyr old). Even if both the lunar and Mercurian heavily cratered terrains were in an empirical saturation equilibrium state, the age difference between the Moon and Mercury would be reduced but Mercury’s NHCT crater retention age would still be post-Nectarian.

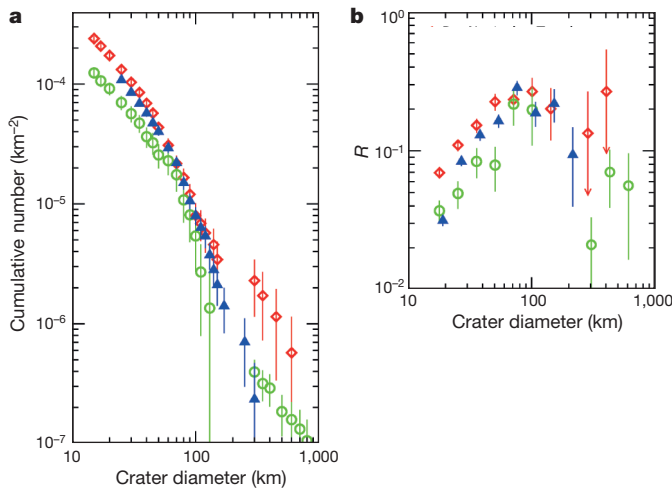


Figure 2 | Comparison of Mercury cratering data with key lunar units. The measured craters on the NHCT (blue triangles) are plotted in a cumulative form (**a**) and on an R -plot (**b**), obtained by normalizing the cumulative size–frequency distributions to a power law D^{-2} , where D is the crater diameter. Pre-Nectarian terrains (red diamonds) encompass a portion of the lunar northern farside^{20,22}. The post-Nectarian crater size–frequency distribution (green circles) was obtained by taking the crater size–frequency distribution (for $D < 300 \text{ km}$) found near or on terrains resurfaced by the formation of Nectaris basin²⁰ and then adding 12 post-Nectaris basins²², all of which had $D > 300 \text{ km}$. Error bars correspond to Poisson statistics.

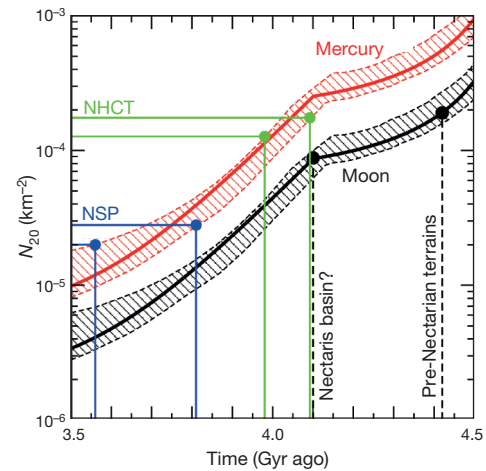


Figure 3 | Mercury and lunar crater chronologies. The solid black curve shows the number of lunar craters larger than 20 km per unit surface (N_{20}), corresponding to the best model⁶. The slope transition at 4.1 Gyr ago marks the onset of the LHB⁶. The inferred age of the pre-Nectarian terrains is also shown, as well as a putative age for the Nectaris basin of 4.1 Gyr (refs 6, 20, 25). The black hatched region represents the envelope of uncertainties in the lunar chronology, as discussed in ref. 6. The Mercury crater chronology (red curve) is obtained by scaling the lunar chronology by a factor of 3. The model uncertainty in the factor of 3 is not considered because it lies within the chronology envelope. The horizontal green lines indicate the range of N_{20} estimated for the NHCT (see Supplementary Fig. 2), which translates into a range of ages spanning from about 4.0 to about 4.1 Gyr ago. The horizontal blue lines indicate the range of N_{20} for the northern smooth plains (NSP; see Supplementary Fig. 2)¹⁶, which translates into a range of ages spanning from about 3.55 to about 3.8 Gyr ago.

We can arrive at a similar conclusion by looking at the record of large basins on the Moon and Mercury (that is, more than 300 km in diameter)⁸. On the Moon there are about 12–15 such basins younger than Nectaris^{22,26}. If the scaling factor derived above is applicable to large LHB-era impactors, which is plausible (see, for example, ref. 25), we would expect about 36–45 basins on Mercury to have accumulated over the same timescale. This number is close to the 46 ± 7 basins (certain and probable) observed on Mercury⁸, and is consistent with our predicted younger age for Mercury's surface. Moreover, the merged large basin size–frequency distribution and NHCT crater size–frequency distribution match remarkably well the model production function over nearly two orders of magnitude in crater sizes (see Supplementary Fig. 4). This strongly suggests that the entire surface of Mercury was resurfaced 4.0–4.1 Gyr ago and that the most ancient crater record (including all visible basins) was produced by impactors having a main belt-like size–frequency distribution.

The end of widespread smooth plains volcanism (see, for example, ref. 16) represents another benchmark in Mercury's history. Using our model production function chronology, we find that the northern smooth volcanic plains¹⁶, which along with the contemporary plains surrounding Caloris basin account for about 17% of the entire surface, were emplaced about 3.55–3.8 Gyr ago (Fig. 3 and Supplementary Fig. 2).

These findings provide compelling evidence for a widespread process, probably volcanism, that erased up to hundreds of millions of years of Mercury's earlier crater history. Moreover, the fact that the globally distributed large basins and the NHCT yield similar ages suggests that the resurfacing was global in nature (see, for example, ref. 10). Our data further indicate that widespread volcanism declined rapidly during the LHB relative to the Moon²⁷, and ended about 3.55–3.8 Gyr ago. After that time, volcanism was much more restricted, occurring only in small patches or within large impact basins²⁸.

Widespread volcanism on Mercury was occurring at the same time as the increase in the impact flux at the start of the LHB period. From an impact statistics point of view, the onset of the LHB was probably followed by a slight delay before the first large basin-forming collisions took place. The fact that our age estimate for Mercury's NHCT is slightly younger than the start of the LHB is consistent with heavy bombardment and basin formation occurring at the same time as global volcanism. Also significant is the cessation of major volcanism near the end of LHB basin formation, thus showing a temporal link between impact flux and volcanism. These findings, coupled with the prediction of a relatively thin lithosphere of Mercury²⁹, support the idea that large impacts may have triggered voluminous volcanism^{30,31}. Vital remaining issues are to what extent and in what ways the impact process had a role in internal melt generation, ascent and eruption.

Received 30 November 2012; accepted 2 May 2013.

1. Strom, R. G. Origin and relative age of lunar and Mercurian intercrater plains. *Phys. Earth Planet. Inter.* **15**, 156–172 (1977).
2. Leake, M. A. *The Intercrater Plains of Mercury and the Moon: their Nature, Origin, and Role in Terrestrial Planet Evolution*. PhD thesis, Univ. of Arizona (1982).
3. Strom, R. G. & Neukum, G. In *Mercury* (eds Vilas, F., Chapman, C. R. & Matthews, M. S.) 336–373 (Univ. Arizona Press, 1988).
4. Neukum, G., Oberst, J., Hoffmann, H., Wagner, R. & Ivanov, B. A. Geologic evolution and cratering history of Mercury. *Planet. Space Sci.* **49**, 1507–1521 (2001).
5. Fassett, C. I. *et al.* The global population of large craters on Mercury and comparison with the Moon. *Geophys. Res. Lett.* **38**, L10202 (2011).
6. Morbidelli, A. *et al.* A sawtooth-like timeline for the first billion years of lunar bombardment. *Earth Planet. Sci. Lett.* **355–356**, 144–151 (2012).
7. Marchi, S. *et al.* A new chronology for the Moon and Mercury. *Astron. J.* **137**, 4936–4948 (2009).

8. Fassett, C. I. *et al.* Large impact basins on Mercury: global distribution, characteristics, and modification history from MESSENGER orbital data. *J. Geophys. Res.* **117**, E00L08, <http://dx.doi.org/10.1029/2012JE004154> (2012).
9. Wilhelms, D. E. Mercurian volcanism questioned. *Icarus* **28**, 551–558 (1976).
10. Strom, R. G. *et al.* Mercury crater statistics from MESSENGER flybys: implications for stratigraphy and resurfacing history. *Planet. Space Sci.* **59**, 1960–1967 (2011).
11. Shoemaker, E. M. *et al.* Interplanetary correlation of geologic time. *Adv. Astronaut. Sci.* **7**, 70–89 (1963).
12. Hartmann, W. K. *et al.* in *Basaltic Volcanism on the Terrestrial Planets* (eds McGetchin, T. R., Pepin, R. O. & Phillips, R. J.) 1049–1127 (Pergamon, 1981).
13. Neukum, G. & Ivanov, B. A. in *Hazards Due to Comets and Asteroids* (eds Gehrels, T., Matthews, M. S. & Schumann, A.) 359–416 (Univ. of Arizona Press, 1994).
14. Stöffler, D. & Ryder, G. Stratigraphy and isotope ages of lunar geologic units: chronological standard for the inner Solar System. *Space Sci. Rev.* **96**, 9–54 (2001).
15. Strom, R. G. *et al.* Mercury cratering record viewed from MESSENGER's first flyby. *Science* **321**, 79–81 (2008).
16. Head, J. W. *et al.* Flood volcanism in the northern high latitudes of Mercury revealed by MESSENGER. *Science* **333**, 1853–1856 (2011).
17. Mainzer, A. *et al.* NEOWISE observations of near-Earth objects: preliminary results. *Astrophys. J.* **743**, 156–173 (2011).
18. Le Feuvre, M. & Wieczorek, M. A. Nonuniform cratering of the Moon and a revised crater chronology of the inner Solar System. *Icarus* **214**, 1–20 (2011).
19. Strom, R. G. *et al.* The origin of planetary impactors in the inner Solar System. *Science* **309**, 1847–1850 (2005).
20. Marchi, S. *et al.* The onset of the lunar cataclysm as recorded in its ancient crater populations. *Earth Planet. Sci. Lett.* **325**, 27–38 (2012).
21. Crater Analysis Techniques Working Group. Standard techniques for presentation and analysis of crater size-frequency data. *Icarus* **37**, 467–474 (1979).
22. Wilhelms, D. E. *The Geologic History of the Moon* (US Geological Survey Professional Paper 1348, 1987).
23. Hartmann, W. K. Does crater 'saturation equilibrium' occur in the solar system? *Icarus* **60**, 56–74 (1984).
24. Bottke, W. F. *et al.* Debiased orbital and absolute magnitude distribution of the near-Earth objects. *Icarus* **156**, 399–433 (2002).
25. Bottke, W. F. *et al.* An Archaean heavy bombardment from a destabilized extension of the asteroid belt. *Nature* **485**, 78–81 (2012).
26. Fassett, C. I. *et al.* Lunar impact basins: stratigraphy, sequence and ages from superposed impact crater populations measured from Lunar Orbiter Laser Altimeter (LOLA) data. *J. Geophys. Res.* **117**, E00H06, <http://dx.doi.org/10.1029/2011JE003951> (2012).
27. Hiesinger, H., Head, J. W., Wolf, U., Jaumann, R. & Neukum, G. in *Recent Advances and Current Research Issues in Lunar Stratigraphy* (eds Ambrose, W. A. & Williams, D. A.) 1–51 (Geological Society of America Special Paper 477, 2011).
28. Marchi, S. *et al.* The effects of the target material properties and layering on the crater chronology: the case of Raditladi and Rachmaninoff basins on Mercury. *Planet. Space Sci.* **59**, 1968–1980 (2011).
29. Smith, D. E. The equatorial shape and gravity field of Mercury from MESSENGER flybys 1 and 2. *Icarus* **209**, 88–100 (2010).
30. Elkins-Tanton, L. T. & Hager, B. H. Giant meteoroid impacts can cause volcanism. *Earth Planet. Sci. Lett.* **239**, 219–232 (2005).
31. Ivanov, B. A. & Melosh, H. J. Impacts do not initiate volcanic eruptions: eruptions close to the crater. *Geology* **31**, 869–872 (2003).

Supplementary Information is available in the online version of the paper.

Acknowledgements The contributions of S.M. and W.F.B. were supported by the NASA Lunar Science Institute (Center for Lunar Origin and Evolution at the Southwest Research Institute in Boulder, Colorado—NASA Grant NNA09DB32A; Center for Lunar Science and Exploration at the Lunar and Planetary Institute in Houston, Texas). S.M. is grateful for being welcomed as a collaborator with the Geology Discipline Group of MESSENGER. C.R.C.'s contribution was supported by the MESSENGER Project. The MESSENGER Project is supported by the NASA Discovery Program under contracts NASW-00002 to the Carnegie Institution of Washington and NAS5-97271 to the Johns Hopkins University Applied Physics Laboratory.

Author Contributions S.M. and C.R.C. performed the new crater measurements. S.M. and W.F.B. computed the impact rates. C.I.F., J.W.H. and R.G.S. provided earlier crater catalogues. All authors contributed to a discussion of the results and their implications, and to writing and revising the manuscript.

Author Information Reprints and permissions information is available at www.nature.com/reprints. The authors declare no competing financial interests. Readers are welcome to comment on the online version of the paper. Correspondence and requests for materials should be addressed to S.M. (marchi@boulder.swri.edu).